Pergamon

PII: S0301-9322(96)00049-3

Int. J. Multiphase Flow Vol. 22, No. 6, pp. 1255–1263, 1996
Copyright © 1996 Elsevier Science Ltd
Printed in Great Britain. All rights reserved
0301-9322/96 $15.00 + 0.00

SHOCKWAVE IN AIR–WATER FLOWS

R. REINAUER and W. H. HAGER
VAW, ETH-Zentrum, CH-8092, Switzerland

(Received 19 November 1995; in revised form 25 June 1996)

Abstract—The effect of air–flow on shockwaves is determined both experimentally and analytically. It is found that model observations conducted with pure water flows may be extended to prototype flow with an aerated flow, by accounting for the mixture shock number. These findings are supported by selected photographs relating to shocks at an abrupt wall deflection. Copyright © 1996 Elsevier Science Ltd.

Key Words: air–water flow, channel flow, oblique jump, shockangle, shockwave

1. INTRODUCTION

Supercritical free surface flows are prone to shockwaves. Those surface waves originate from external disturbances, such as changes:

- in the channel alignment away from the straight wall direction,
- of the bottom geometry away from the plane invert,
- of discharge, i.e. either addition or reduction of discharge, or
- of boundary roughness.

Hydraulic jumps are a particular type of shocks with a shock front perpendicular to the flow direction. The classical hydraulic jump is the basic jump type in a rectangular horizontal channel with an inviscid fluid. Both strong classical hydraulic jumps and shocks may break, resulting in a surface return flow with a considerable local air entrainment at the interface between forward bottom and return surface flows. The significant difference between the classical hydraulic jump and the shockwave as considered here is energy dissipation. For shockwaves, energy dissipation is negligible, whereas hydraulic jumps are applied as energy dissipators due to their intensive energy consumption.

Chute flow that is originally undisturbed will remain invariant only in a straight and prismatic channel with a constant roughness and discharge. Such idealized conditions are often impossible due to boundary constraints. The basic disturbance of supercritical flow, i.e. where the so-called Froude number $\mathbf{F} = V/c$ and V = average velocity, and c = celerity is in excess of unity corresponds to the abrupt wall deflection. The abrupt wall deflection is amenable to analysis provided effects of friction and bottom slope are neglected. A detailed analysis is given below.

The present project was conducted to obtain insight in a typical model effect. Whereas free surface flow in a prototype chute is usually aerated due to surface aeration, hydraulic models have usually flows, of which the velocity is too small for incipient surface aeration. The question thus is how shockwaves behave under preaerated flow conditions. More specifically: are the heights of shockwaves in a prototype situation larger or smaller than the heights in the corresponding hydraulic model? Both, yes and no have some support. A height of shockwave can be larger in the prototype because of the mixture flow, and a shockwave is eventually damped by the presence of air, and thus may be lower in the prototype. The present study was undertaken to answer this question, based on previous observations of shockwaves in pure water flow. The answer to the problem is so simple and significant at the same time that the results were considered worth publishing in the Journal.

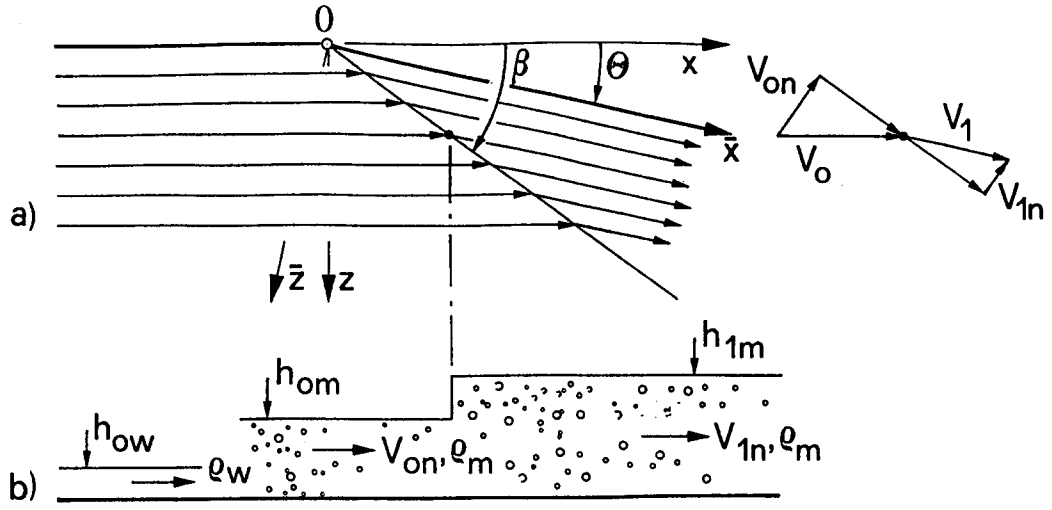

Figure 1. Definition of flow across an abrupt wall deflection (a) plan, (b) side view.

2. MIXTURE QUANTITIES

The abrupt wall deflection involves the basic configuration for a shockwave. Consider a homogeneous two-phase flow of approach (index o) flow depth h_{om}, approach density ρ_{om} and approach velocity V_{om}. The flow is bounded by a straight wall that is deflected by the angle θ at point O (figure 1). For simplicity we consider a rectangular channel with a hydraulically smooth boundary and a horizontal channel containing an air–water flow where there is no slip of the air bubbles. The roughness effect could be accounted for by a more complex formulation that is omitted for conciseness here (Reinauer 1995). Quantities relating to pure water are referred to with subscript w, and m indicates air–water mixture parameters.

Due to the wall deflection angle θ a shock front of shock angle β results, and quantities beyond the front are designated with subscript 1. The mechanism of a shock in one-phase flow is well understood, based on the continuity and the momentum equations parallel and perpendicular to the front (Ippen 1951). We ask as to how the shock formation is modified by the addition of air to the water flow.

With index a referring to air the mean air concentration C is defined as

$$C = \frac{Q_a}{Q_a + Q_w} = \frac{Q_a}{Q_m}. \qquad [1]$$

The mean mixture flow depth h_m is related to the water flow depth

$$h_m = h_w/(1 - C). \qquad [2]$$

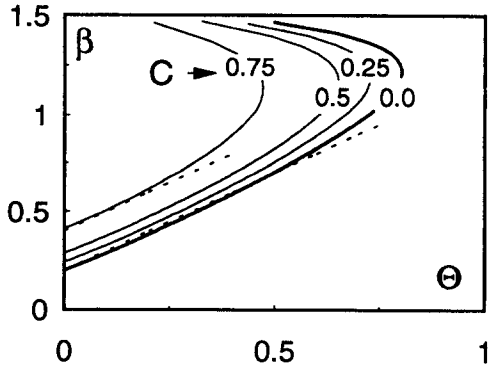

Figure 2. Shock angle β as a function of deflection angle θ for various air concentrations C. (—) [14]. $F_{om} = 5$.

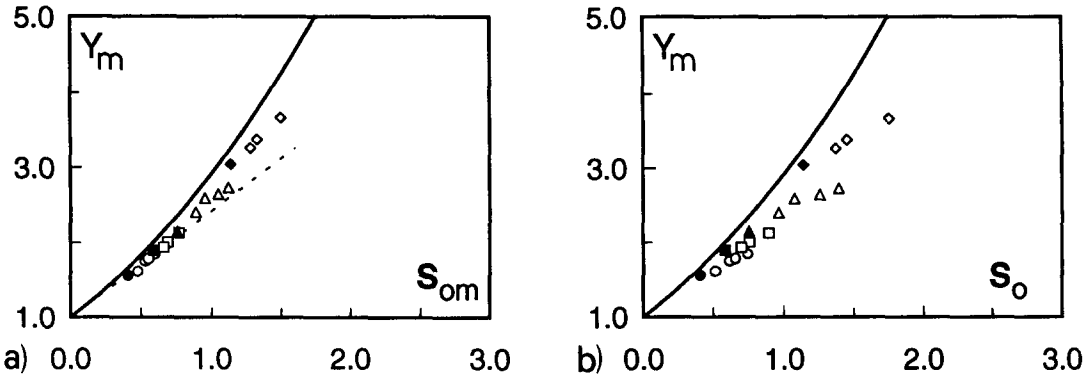

Figure 3. Mixture flow depth Y_m as a function of (a) mixture approach shock number S_{om}, (b) shock number S_o. (——) Prediction according to [17], (· · · ·) first order approximation [15].

With g as gravitational acceleration, and when accounting for $\rho_m = \rho_w(1 - C)$ from [1] the bottom pressure p_m of a mixture flow is

$$p_m = \rho_m g h_m = \rho_w(1 - C)g \frac{h_w}{(1 - C)} = \rho_w g h_w. \quad [3]$$

The corresponding hydrostatic pressure force $P_m = (1/2)p_m h_m$ is, therefore,

$$P_m = \rho_w g \frac{h_w^2}{2(1 - C)}. \quad [4]$$

This is in agreement with the result of Herbrand (1969).

The momentum M of a mixture flow is $M_m = \rho_m V_m Q_m$. Assuming no relative velocity between air bubbles and water particles yields $V_a = V_w = V_m$ in a flow without pressure gradient. Because $\rho_m = \rho_w(1 - C)$ and $Q_m = Q_w/(1 - C)$ one has the simple result

$$M_m = \rho_w(1 - C)V_w \frac{Q_w}{(1 - C)} = \rho_w V_w Q_w. \quad [5]$$

The momentum of a mixture flow is thus equal to the momentum of the pure water flow of equal velocity and discharge (Herbrand 1969).

3. SHOCK EQUATIONS

Consider figure 1 with a mixture approach flow (ρ_m, Q_m, h_{om}) across a wall deflection. Beyond the shock front the quantities of interest are the mixture flow depth h_{1m} and the shock angle β. Preliminary observations indicated that the velocity across a shock remains constant and this may also be substantiated with the asymptotic set of equations by Ippen (Hager *et al.* 1994).

When accounting for [4] and [5] the momentum equation normal (subscript n) to the shock front is

$$\tfrac{1}{2}\rho_w g \frac{h_{ow}^2}{(1 - C)} + \rho_w h_{ow} V_{on}^2 = \tfrac{1}{2}\rho_w g \frac{h_{1w}^2}{(1 - C)} + \rho_w h_{1w} V_{1n}^2. \quad [6]$$

From a vector diagram V_n can be related to the absolute value of velocity V both up- and downstream of the shockfront (figure 1). Dividing by $(\rho_w g)$ yields

$$\frac{1}{2}\frac{h_{ow}^2}{(1 - C)} + \frac{h_{ow}}{g} V_o^2 \sin^2 \beta = \frac{1}{2}\frac{h_{1w}^2}{(1 - C)} + \frac{h_{1w}}{g} V_{1w}^2 \sin^2(\beta - \theta). \quad [7]$$

Introducing $V_{ot} = V_{1t}$ in the tangential (subscript t) direction and the continuity equation

$$V_{on} h_{ow} = V_{1n} h_{1w} \quad [8]$$

gives further

$$\frac{\sin(\beta - \theta)}{\sin \beta} = \frac{V_o}{V_1} \frac{h_{ow}}{h_{1w}}. \quad [9]$$

The mixture Froude number in a rectangular channel is $\mathbf{F}_m = V_m/(gh_m)^{1/2} = [V_w/(gh_w)^{1/2}](1 - C)^{1/2}$. Because of the no-slip assumption, the depth ratio $Y = h_1/h_o$ is, with [7]

$$1 + 2\mathbf{F}_{om}^2 \sin^2 \beta = Y_m^2 + 2\mathbf{F}_{om}^2 Y_m \sin^2(\beta - \theta). \quad [10]$$

Using [9] to eliminate $\sin(\beta - \theta) = Y_w^{-1} \sin \beta = Y_m^{-1} \sin \beta$ gives

$$1 + 2\mathbf{F}_{om}^2 \sin^2 \beta = Y_m^2 + 2\mathbf{F}_{om}^2 Y_m^{-1} \sin^2 \beta. \quad [11]$$

By excluding the trivial solution $Y_m = 1$ yields a quadratic equation for Y_m with the physically relevant solution

$$Y_m = \tfrac{1}{2}[(1 + 8\mathbf{F}_{om}^2 \sin^2 \beta)^{1/2} - 1]. \quad [12]$$

For large values of $\mathbf{F}_{om} \sin \beta$ this approximates as

$$Y_m = \sqrt{2}\mathbf{F}_{om} \sin \beta - \tfrac{1}{2}, \quad [13]$$

in agreement with previous results for water flow (Hager 1992).

The shock angle β may be obtained from [9] and [13] when eliminating Y_m. For small angles $\sin \beta \cong \beta$, and

$$\beta - \theta = \frac{3}{2\sqrt{2}\mathbf{F}_{om}} \cong \frac{1}{\mathbf{F}_{om}}. \quad [14]$$

Inserting this result back into [13] yields to the same order

$$Y_m = 1 + \sqrt{2}\theta\mathbf{F}_{om}. \quad [15]$$

Equations [14] and [15] are the basic equations for supercritical flow across an abrupt wall deflection. They are, at least to lowest order of approximation, exactly identical with the water flow equations, except that $Y \rightarrow Y_m$ and $\mathbf{F}_o \rightarrow \mathbf{F}_{om}$. The height of shock is increasing linearly with the deflection angle θ, and the mixture Froude number $\mathbf{F}_{om}$. Based on this simple result, Hager *et al.* (1994) introduced the *approach shock number* $\mathbf{S}_o$. For mixture flow, one may extend its definition as

$$\mathbf{S}_{om} = \theta\mathbf{F}_{om}. \quad [16]$$

The ratio of mixture shock flow depth to mixture approach flow depth thus depends exclusively on the *mixture shock number* $\mathbf{S}_{om}$. Also, the shock angle ratio $\sigma = (\beta/\theta) - 1 = (\mathbf{S}_{om})^{-1}$ depends exclusively on $\mathbf{S}_{om}$. Figure 2 shows the solution for the shock angle β as a function of θ for various air concentrations C, according to the full equation [9]. Also plotted is the approximation [14] for $C = 0$, and $C = 0.75$, and both are valid up to $\theta = 0.25$, corresponding to $\theta = 14°$. Such a deflection angle is known to be rather large and at the upper limit of engineering application.

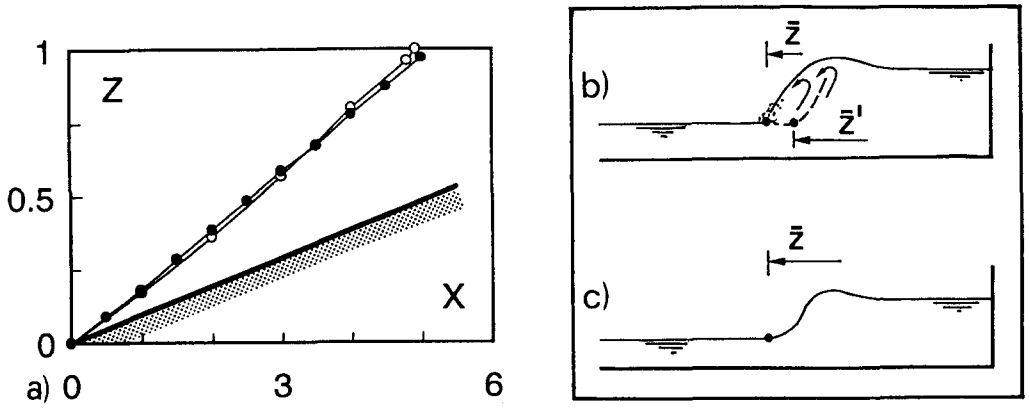

Figure 4. (a) Shock front $Z(X)$ for (●) pure water and (○) mixture flow with $\mathbf{F}_o = \mathbf{F}_{om} = 6.17$, definition of shock front, (b) breaking front for strong shock, (c) compact front for weak shock.

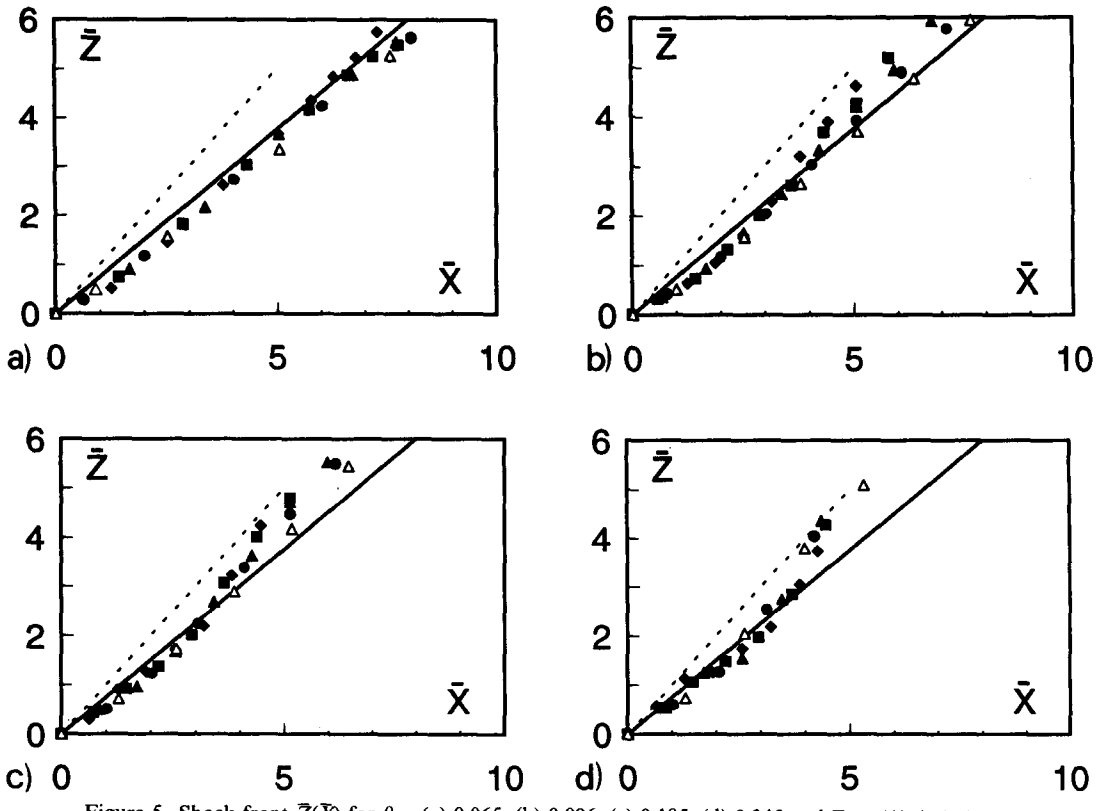

Figure 5. Shock front $\bar{Z}(\bar{X})$ for θ = (a) 0.065, (b) 0.096, (c) 0.185, (d) 0.345 and F_o = (Δ) 4, (●) 5, (▲) 6, (■) 7 and (◆) 8. (——) γ=0.75, (· · · ·) γ = 1.

4. EXPERIMENTAL RESULTS

The experimental verification of the previous results was conducted in a 500 mm wide rectangular channel. The transition from the pressurized pipe to the open channel flow involved a jet-box, i.e. an element containing diffusors and flow straighteners with an approach flow of predetermined height h_o up to 100 mm of accuracy ± 0.5 mm. The quality of the approach flow was excellent both in terms of uniformity and disturbances. Based on previous experimentation (Reinauer 1995) an approach flow depth of $h_o = 50$ mm was chosen to inhibit scale effects. Because the significance of the shock number was known from earlier analysis, only two deflection angles $\theta = 0.096$, and $\theta = 0.186$ were set, and S_o was varied by increasing F_{ow} from 4.07 to 9.42.

Air was added 5 m upstream from the jet-box to the pipe, and turbulence diffused it over the entire pipe section to result in a homogeneous bubbly liquid. The air discharge Q_a was determined with a WISAG 2000 air meter, connected to a pressure cell to $\pm 2.5\%$. The water discharge was metered with an Inductive Discharge Measurement (IDM) device to $\pm 1.5\%$, or 1 l s^{-1}, whichever is larger. At the approach section of the channel, the air and water discharges, and the mixture flow depth h_{om} were thus known, and the mixture shock number S_{om} could be computed. The bottom slope of the channel was adjusted to 10° such that there was nearly no acceleration nor deceleration of the flow, and the friction slope was compensated for by the bottom slope, as previously assumed for our simplified model (Reinauer and Hager 1996).

Shock height

The mean air concentration C as defined in [1] was varied between 0 and 0.37 (37%), and mixture shock numbers S_{om} between 0.4 and 1.5 were considered. Figure 3(a) shows the shock height ratio $Y_m = h_{1m}/h_{om}$ as a function of S_{om} and indicates perfect similarity for all runs. Also plotted is the zero-order approximation [15] and the relative wave height as obtained by Reinauer (1995) for water flow alone

$$Y = \left(1 + \frac{1}{\sqrt{2}} \mathbf{S}_o\right)^2. \qquad [17]$$

Note that the first approximation of [17] is $Y = 1 + \sqrt{2}\mathbf{S}_o$, in agreement with [15] for mixture flow. The data are located somewhat below [17] because the deaeration process along the shockfront. In the experiments air was added by the approach pipe, but the velocity of flow (up to 5 ms^{-1}) was too small for surface aeration to occur.

Figure 3(b) shows a conventional plot $Y_m(\mathbf{S}_o)$ and indicates a considerable scatter of data when using the shock number $\mathbf{S}_o = \theta\mathbf{F}_o$ instead of $\mathbf{S}_{om} = \theta\mathbf{F}_{om}$ for mixture flow. The novel approach accounts for the two-phase flow in a simple and effective manner, therefore.

The geometry of the shockfront was observed for a selected run, where $\theta = 0.096$, $Q_w = 56.4$ l s^{-1} and $\mathbf{F}_o = 6.17$. For water flow alone ($C = 0$) the approach flow depth was $h_o = 32.4$ mm, for mixture flow with $C = 0.325$, the discharge was 70 l/s and the mixture flow depth was determined from [2] to $h_{om} = 50$ mm and $\mathbf{F}_{om} = 6.17$ also. It is seen from figure 4(a) that the shock fronts match almost exactly, and that [14] is a simple extension for the shock angle.

Shock front

When comparing the shock angle from figure 4(a) with [14] a systematic deviation may be stated. This is not only due to the neglect of higher order terms but also because of curvature effects. In order to define a shock front more exactly, additional experiments in a horizontal smooth channel were conducted, where $\theta = 0.065$, 0.096, 0.185 and 0.345, and $\mathbf{F}_o = 4$–8 with increments of 1. The approach flow depth was $h_o = 50$ mm throughout, and pure water flow was used because of increased accuracy in defining the front geometry. Based on previous work by Schwalt & Hager (1992) where the shock surface geometry was studied, we examined the shock front geometry here.

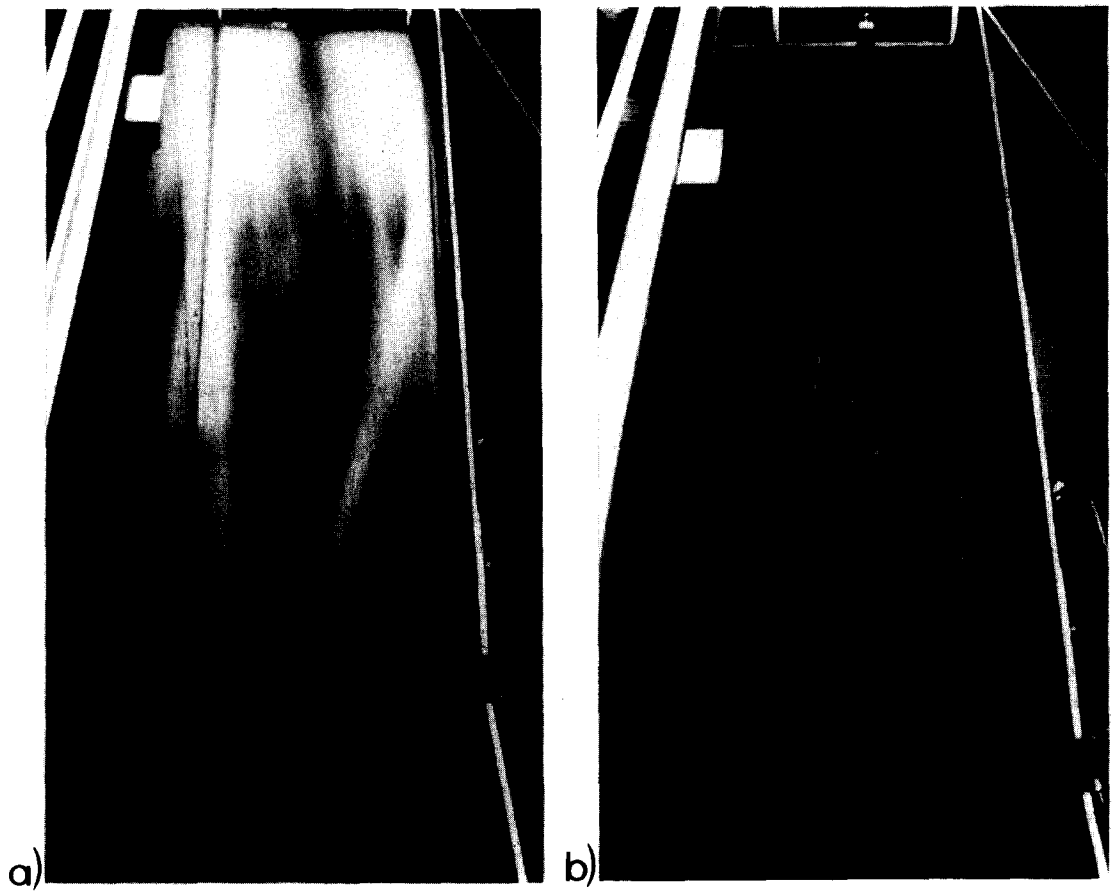

Figure 6. Overall view of shockwave for $\mathbf{S}_o = \mathbf{S}_{om} = 6.17$, (a) mixture and (b) water flow.

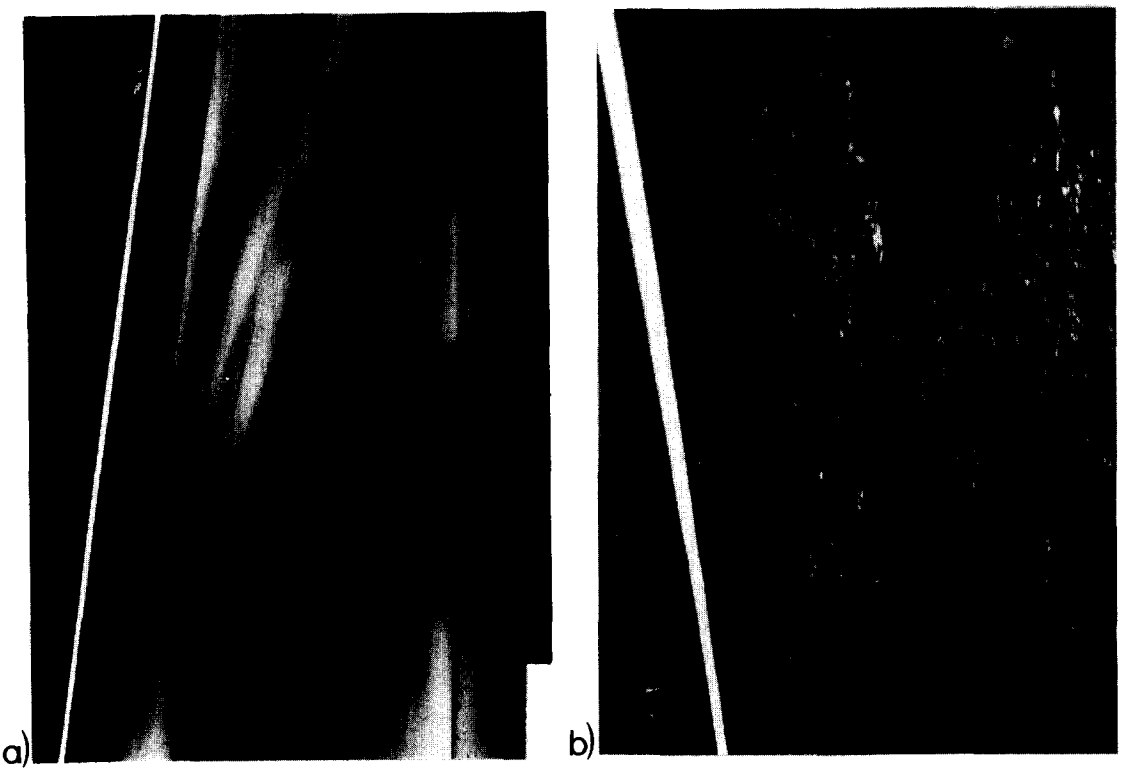

Figure 7. Details of shockwaves, (a) mixture and (b) water flow.

Two cases must be distinguished (figure 4(b, c)): For small shock number, the front remains compact and may easaily be defined. For larger shock number, a surface roller is formed as for a classical hydraulic jump. The fluid coming transversally onto the front is able to "clear" the roller flow, however, and the extension of the surface roller in a breaking shock is much smaller than for a corresponding hydraulic jump.

Based on a coordinate system $(\bar{x}, \bar{z})$ as defined in figure 1, with origin at the deflection point O and directed along the deflected wall, one may plot the relative shock front $\bar{Z}(\bar{X})$, where $\bar{X} = x/(h_o \mathbf{F}_o)$ is a so-called Rouse coordinate, and $\bar{Z} = \bar{z}/h_o$ (Hager 1992). Figure 5 shows that for a specific deflection angle θ, the data for various Froude numbers $\mathbf{F}_o$ are similar. Also the data for various θ are scattering around a straight curve

$$\beta - \theta = \frac{\gamma}{\mathbf{F}_o} \qquad [18]$$

where $\gamma = 0.75$. Further, the theoretical curve [14] with $\gamma = 1$ is plotted, and this shock angle is seen to be too large, although the data approach the dotted line for large $\bar{X}$. This is due to the wave breaking phenomenon mentioned previously, starting at about $\bar{X} = 4$, provided $Y \geqslant 2$. The important feature of figure 5 is that, for both pure water and mixture flow, the shock front may be expressed from [18] as

$$\sigma_m = (\beta_m/\theta) = 1 + \frac{0.75}{\mathbf{S}_{om}}. \qquad [19]$$

Accordingly, the shock angle ratio depends exclusively on the mixture shock number, as do all other properties of shock flow.

Photographs

Photographs were made to allow a comparison between aerated and non-aerated flows across a shock. The hydraulic conditions as stated previously were taken, i.e. $\mathbf{F}_o = \mathbf{F}_{om} = 6.17$, and $\theta = 0.096$ such that $\mathbf{S}_o = \mathbf{S}_{om} = 0.60$. Figure 6 refers to a view against the flow and one may see

a well-defined front for the pure water flow, whereas the mixture flow has a less sharp front geometry, due to the high air concentration. The pressure at the front has a strong gradient, and is not hydrostatic. In the upstream front portion, there is an overpressure due to streamline curvature with center above the flow (figure 4(c)) and vice versa slightly downstream. The air bubbles are thus first lifted due to increased buoyancy and escape into the atmosphere. The shock front is thus perfectly traced by air bubbles, and the air concentration beyond the front is strongly reduced. Tracing the pattern of a supercritical flow is thus simply achieved by adding some air to the approach flow.

A detail of the shockfront in the direction of flow is seen in figure 7, both for mixture and pure water flows. Note the abrupt deflection of surface streamlines across the front and the step increase of flow depth. The pattern of streamlines are visible by long time exposure of 1/30 s.

Tailwater views from the shockwaves are provided by figure 8. In Figure 8(a) the effect of deaeration across a shock is highlighted, whereas figure 8(b) reveals the initial curvature of shock front, away from the point of deflection. One may also see the step increase of flow and the nearly constant wall flow depth, as determined with [15]. Just downstream of the deflection point O, the flow is unable to react immediately to the deflection in the plan view, and there is a superelevation along the wall, therefore (Hager *et al.* 1994). The lateral expansion of flow is confined to the zone downstream of the superelevation, as is also recognized from figure 5.

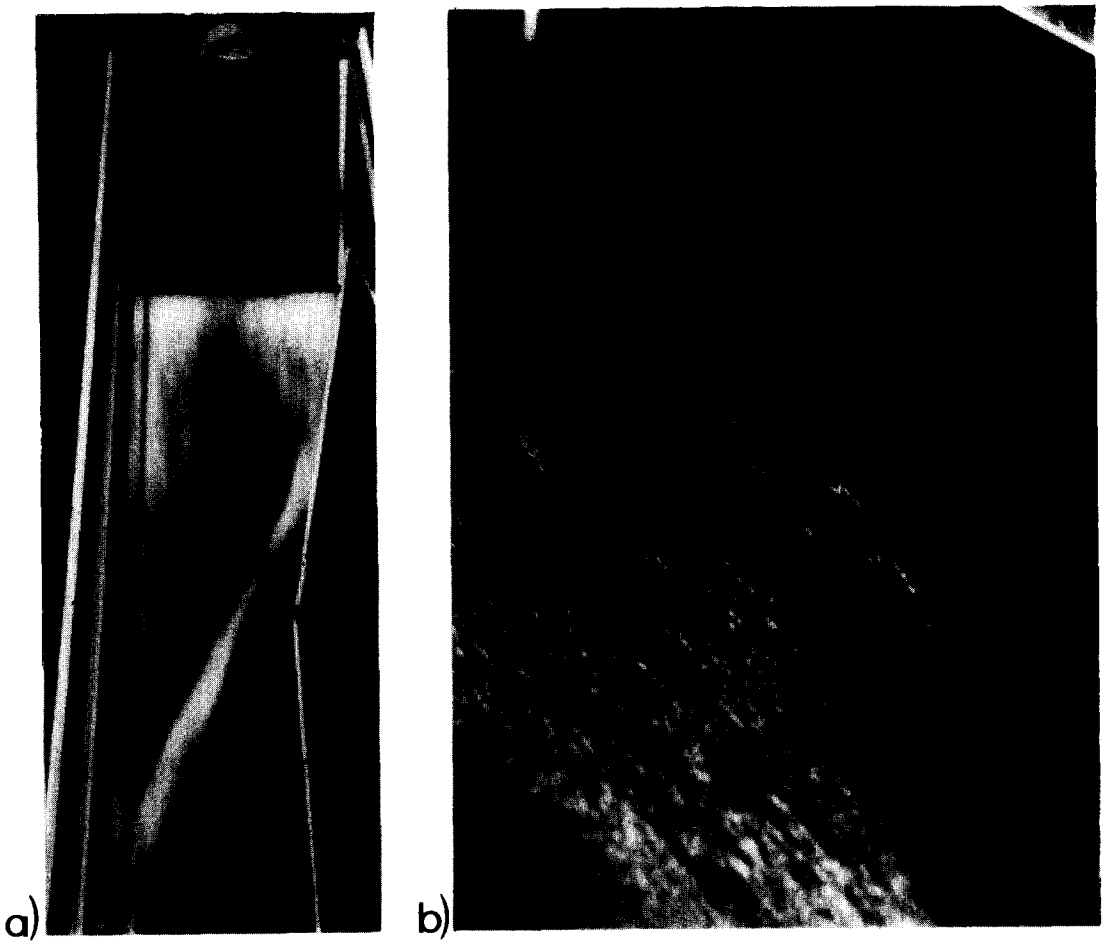

Figure 8. Tailwater views of shockwave, (a) mixture and (b) water flow.

5. CONCLUSIONS

The mechanism of air–water flow across an abrupt wall deflection is studied. The 2D approach demonstrates that the relations as derived for one-phase flow may be expanded to two-phase flow provided mixture quantities instead of pure water quantities are accounted for. This concept may be expanded for arbitrary supercritical flows, because of the relative insignificance of pressure forces when compared to the inertial forces in the approach flow.

The theoretical approach was verified with selected experiments in a horizontal and a sloping smooth rectangular channel. It was found that the shock fronts are identical for equal mixture shock numbers. Also the geometry of shock fronts was determined in pure water flows. The concept of shock number was verified for both mixture and water flows, and identified as the governing flow parameter.

The findings were documented with selected photographs. These indicate that a shock front can be considered as a localized deaerator, and that shock fronts clearly trace the flow pattern when adding air to the approach flow.

REFERENCES

Hager, W. H. 1992 Spillways—shockwaves and air entrainment. *ICOLD Bulletin*, Vol. 81, International Commission on Large Dams, Paris.

Hager, W. H., Schwalt, M., Jimenez, O. & Chaudhry, M. H. 1994 Supercritical flow near an abrupt wall deflection. *Journal of Hydraulic Research* **32,** 103–118.

Herbrand, K. 1969 Der Wechselsprung unter dem Einfluss der Luftbeimischung (The hydraulic jump under the influence of air addition). *Wasserwirtschaft* **59,** 254–260 (in German).

Ippen, A. T. 1951 Mechanics of supercritical flow. *Trans. ASCE* **116,** 268–295.

Reinauer, R. 1995 Kanalkontraktion bei schiessendem Abfluss und Stosswellenreduktion mit Diffraktoren (Chute contraction for supercritical flow and shock reduction with diffractors). Ph.D. thesis number 11320. Swiss Federal Institute of Technology, Zurich (in German).

Reinauer, R. & Hager, W. H. 1995 Generalized drawdown curve for chutes. *Proc. Institution Civil Engineers Water, Maritime and Energy* **118,** 196–198.

Schwalt, M. & Hager, W. H. 1992 Analysis of shock wave. *Water Forum '92 ASCE National Conference*, Baltimore, pp. 231–236.